© 2016. Published by The Company of Biologists Ltd | Development (2016) 143, 2898-2906 doi:10.1242/dev.134411

STEM CELLS AND REGENERATION

RESEARCH ARTICLE

Satellite cell depletion prevents fiber hypertrophy in skeletal muscle

Ingrid M. Egner[1], Jo C. Bruusgaard[1,2] and Kristian Gundersen[1,*]

ABSTRACT

The largest mammalian cells are the muscle fibers, and they have multiple nuclei to support their large cytoplasmic volumes. During hypertrophic growth, new myonuclei are recruited from satellite stem cells into the fiber syncytia, but it was recently suggested that such recruitment is not obligatory: overload hypertrophy after synergist ablation of the plantaris muscle appeared normal in transgenic mice in which most of the satellite cells were abolished. When we essentially repeated these experiments analyzing the muscles by immunohistochemistry and *in vivo* and *ex vivo* imaging, we found that overload hypertrophy was prevented in the satellite cell-deficient mice, in both the plantaris and the extensor digitorum longus muscles. We attribute the previous findings to a reliance on muscle mass as a proxy for fiber hypertrophy, and to the inclusion of a significant number of regenerating fibers in the analysis. We discuss that there is currently no model in which functional, sustainable hypertrophy has been unequivocally demonstrated in the absence of satellite cells; an exception is re-growth, which can occur using previously recruited myonuclei without addition of new myonuclei.

KEY WORDS: Hypertrophy, Plasticity, Satellite cells, Skeletal muscle, Stem cells, Mouse

INTRODUCTION

Size matters in skeletal muscle because force is proportional to cross-sectional area and mass to power. Muscle mass can vary considerably, and is modified by hormones, disuse, strength exercise or experimental overload (Egner et al., 2013; Eriksson et al., 2005; Gundersen, 2011; Herbst and Bhasin, 2004). Muscle mass is mainly altered by changing the size of pre-existing muscle fibers, and fiber loss or *de novo* formation of fibers is believed to play a much lesser role (Allen et al., 1999; Gollnick et al., 1981; MacDougall et al., 1984; Taylor and Wilkinson, 1986; White et al., 2010).

During hypertrophy each fiber displays radial growth, and it has been believed that the number of myonuclei in each fiber syncytium increases by satellite cells multiplying and fusing with the muscle fibers in order to support the larger cytoplasmic volume. It is well-documented that new myonuclei are recruited in this way during many hypertrophic conditions (Allen et al., 1995, 1999; Aloisi et al., 1973; Bruusgaard et al., 2010; Cabric et al., 1987; Cabrić and James, 1983; Cheek et al., 1971; Enesco and Puddy, 1964; Giddings and Gonyea, 1992; Kadi et al., 1999; Lipton and Schultz, 1979; McCall et al., 1998; Moss, 1968; Moss and Leblond, 1970; Roy et al., 1999; Schiaffino et al., 1976; Seiden, 1976; Winchester and Gonyea, 1992), and recruitment of myonuclei seems to precede the radial growth (Bruusgaard et al., 2010), thus a causal role is suggestive.

Attempts to prevent satellite cell activity by blocking DNA synthesis by γ-irradiation (Adams et al., 2002; Barton-Davis et al., 1999; Phelan and Gonyea, 1997; Rosenblatt and Parry, 1992; Rosenblatt et al., 1994) have suggested that proliferation of satellite cells is necessary for efficient hypertrophic growth. There have, however, been some conflicting reports (Lowe and Alway, 1999; Rosenblatt and Parry, 1993), and the specificity of the γ-irradiation for cell proliferation has been questioned (McCarthy and Esser, 2007).

The necessity of recruiting new myonuclei was directly challenged by McCarthy et al. (2011) who utilized a mouse strain with an IRES cassette in which *Pax7* promoter elements drive expression of Cre-recombinase in the presence of tamoxifen crossed to a strain with a floxed diphtheria toxin A expression vector. This model yields mice in which most of the satellite cells are ablated when tamoxifen is administered.

In such animals, they subjected the plantaris muscle to overload (OL+) by ablation of the synergistic soleus and gastrocnemius muscles. They reported that there was little difference in the hypertrophic response in the satellite-deficient mice (SC−) compared with controls with intact satellite cells (SC+). Based on these findings, they conclude that they 'provide convincing evidence that skeletal muscle fibers are capable of mounting a robust hypertrophic response to mechanical overload that is not dependent on satellite cells'.

In the present study, we essentially repeated the experiments of McCarthy et al. (2011), but our data failed to support their conclusions. We observed a robust overload hypertrophy in the plantaris in SC+ mice, whereas in SC− mice hypertrophy was prevented. Similar experiments on the extensor digitorum longus (EDL) gave essentially the same result. Based on our data, we conclude that the hypertrophic response to mechanical overload is dependent on satellite cells.

RESULTS

Tamoxifen efficiently ablated satellite cells in overloaded muscles

In order to investigate the efficiency of the satellite cell ablation after administration of tamoxifen, the number of Pax7$^+$ cells was counted on whole mid-belly cross-sections from plantaris muscles (Fig. 1A).

The crucial observation was that the absolute number of Pax7$^+$ cells in the tamoxifen-treated SC−OL+ mice remained low (Fig. 1A), as the average number of Pax7$^+$ cells per cross-section (5.2) was similar to that found in normal SC+OL− mice (5.0; Fig. 1B). This finding was similar to the observations of McCarthy et al. (2011).

[1]Department of Biosciences, University of Oslo, Blindern, Oslo N-0316, Norway. [2]Department of Health Sciences, Kristiania University College, P.O. Box 1190, Sentrum, Oslo N-0107, Norway.

*Author for correspondence (kgunder@ibv.uio.no)

J.C.B., 0000-0001-8163-5849; K.G., 0000-0001-9040-3126

Received 23 December 2015; Accepted 28 June 2016

Development (2016) 143, 2898-2906 doi:10.1242/dev.134411

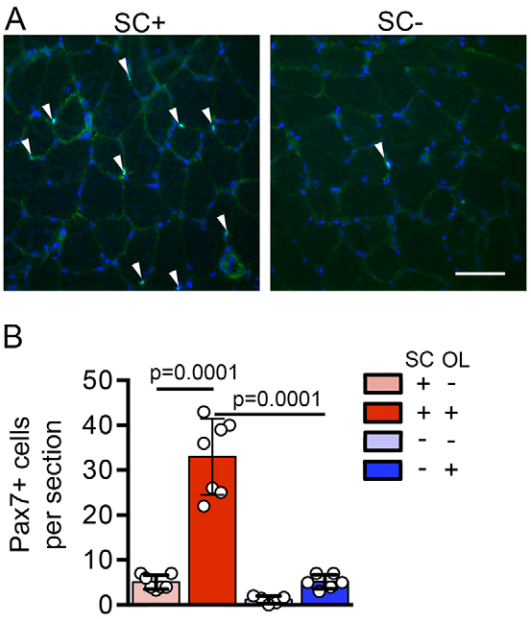

Fig. 1. The effect of tamoxifen treatment and overload on the number of Pax7$^+$ cells in plantaris muscles. (A) Micrographs of cryosections from SC+ OL+ (left) and SC−OL+ (right) plantaris muscles stained for DNA (blue) and Pax7 (green). Arrowheads indicate Pax7$^+$ nuclei. Scale bar: 50 µm. (B) The number of Pax7+ cells identified on whole mid-belly cross-sections of the plantaris muscle is given as mean±s.e.m., and values from individual animals (circles). SC+OL− *n*=7; SC+OL+ *n*=7; SC−OL− *n*=5; SC−OL+ *n*=6.

The number of Pax7$^+$ cells in SC− mice was 24% of that of SC+ controls without overload (Fig. 1B). After overload, the number of Pax7$^+$ cells in SC+ control mice increased by 650%, which was a stronger activation than that observed by McCarthy et al. (2011). In our SC− mice, overload led to a 420% increase, indicating that satellite activation took place, but resulting in a much smaller absolute number of Pax7$^+$ cells in the tamoxifen-treated mice than in SC+ mice.

Functional overload of the plantaris but not EDL can lead to significant muscle damage

Overload by synergist ablation is a rather invasive procedure, particularly for the plantaris. The sudden load put on the muscle is high, as it has to bear the load of the large triceps surae complex. Also, the blood supply to the plantaris that passes through the gastrocnemius is prone to damage during the ablation. In our material, five out of the 30 muscles that were ablated were almost completely degenerated, and were excluded from further analysis.

All individual muscles were investigated for central nuclei and labeling for embryonic myosin (Myh3) as markers of regenerating fibers (Fig. 2). In non-overloaded (OL−) plantaris muscles, only 0.7 and 1.4% of the fibers showed one or both of these signs in the SC− and SC+ group, respectively (Fig. 2D, left-hand graph). This increased to 4% and 13% after overload (OL+). For the latter group, the variability was high, ranging from 2 to 23%.

In the EDL, damage and regeneration seemed to be less of a problem (Fig. 2, right panels). The average number of fibers with embryonic myosin and/or central nuclei was below 1.5% in all experimental groups and in no single muscle did more than 5% of the fibers display such signs. Nonetheless, these fibers were excluded from our hypertrophy analysis.

Since we suggest below that the inclusion of regenerating fibers might be a confounding factor if included in the analysis of hypertrophy such as by McCarthy et al. (2011), it was of interest to

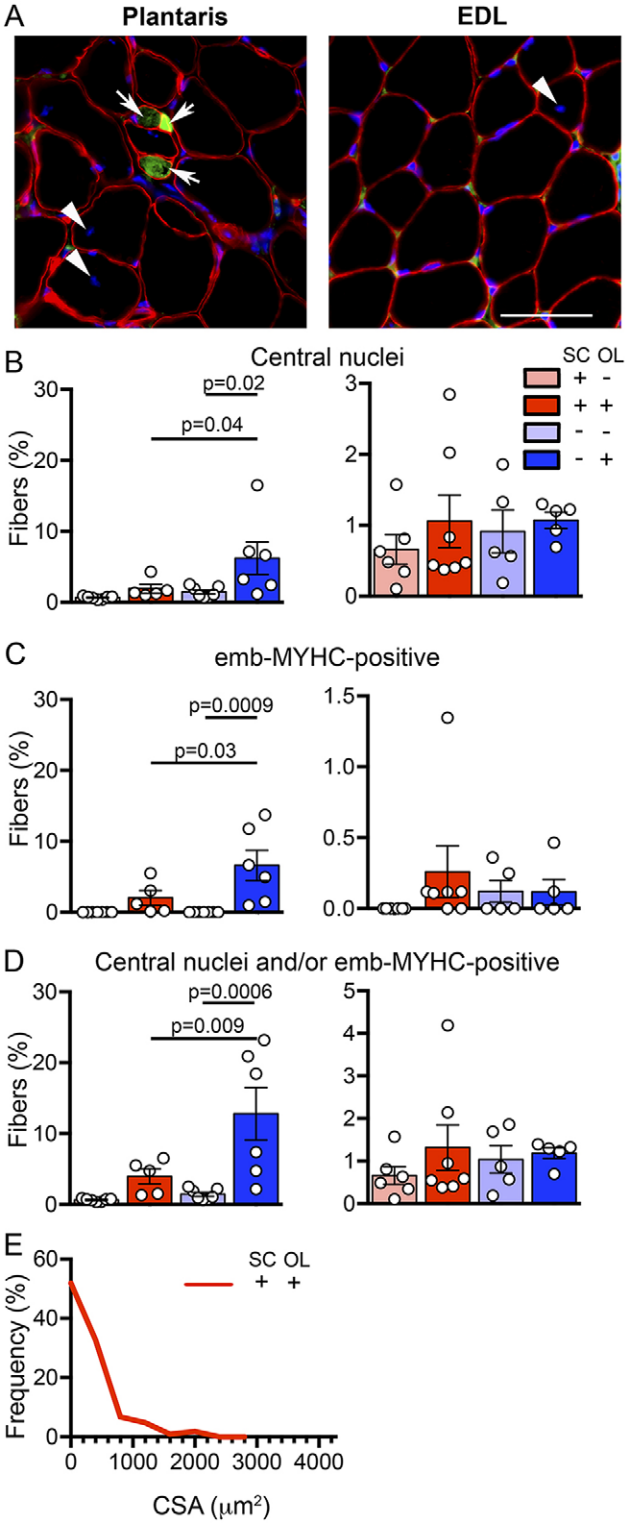

Fig. 2. The effect of overload on damage and/or regeneration markers. (A) Micrographs of cryosections from overloaded plantaris (left) and EDL (right) muscles stained for DNA (blue), laminin (red) and embryonic myosin (green). Scale bar: 50 µm. White arrows indicate fibers positive for MYH3 staining; arrowheads indicate fibers with central nuclei. (B-D) Quantification of fibers with central nuclei (B), embryonic myosin (C) or at least one of these characteristics (D) in plantaris (left panels) and EDL (right panels). Data are given as mean±s.e.m., and the values from individual animals (circles). SC+OL− *n*=6; SC+OL+ *n*=7; SC−OL− *n*=5; SC−OL+ *n*=6. (E) CSA distribution of regenerating fibers in SC+OL+ plantaris muscles (*n*=103 fibers from three animals).

Development (2016) 143, 2898-2906 doi:10.1242/dev.134411

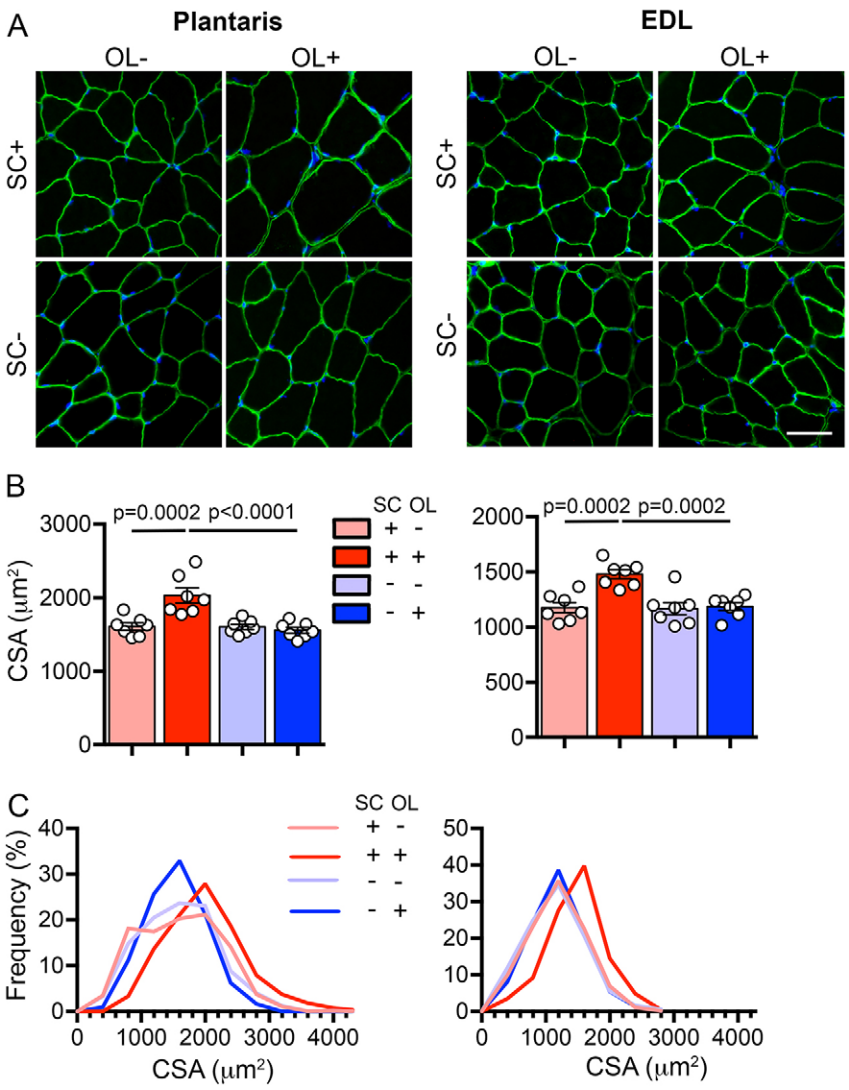

Fig. 3. The effect of overload on fiber CSA. (A) Micrographs of cryosections from plantaris (left panels) and EDL (right panels), stained for DNA (blue) and dystrophin (green). Scale bar: 30 µm. (B) Average CSA values from individual muscles (circles), and mean± s.e.m. for each experimental group of plantaris (left panels) and EDL (right panels). *n*=7 animals in each group. (C) CSA distribution of all fibers measured for each experimental group from plantaris (left panel) and EDL (right panel). Plantaris: SC+OL− *n*=1004; SC+OL+ *n*=936; SC−OL− *n*=900; SC−OL+ *n*=911 fibers. EDL: SC+OL− *n*=929; SC+OL+ *n*=976; SC−OL− *n*=1083; SC−OL+ *n*=873 fibers.

study the cross-sectional area (CSA) of this population separately. We had a low number of such fibers, but CSA was measured in 103 fibers from three plantaris muscles from SC+OL+ mice. These fibers had an average CSA of 334 µm^2 and the complete size distribution is given in Fig. 2E.

Satellite cell ablation prevents overload hypertrophy

Based on histological observations of cryosections (Fig. 3A), in SC+ muscles overload led to 26% increase in CSA in both the plantaris and the EDL. By contrast, overload had essentially no effect on average CSA in SC− muscles in either of the two muscles (Fig. 3B). There was no significant effect on average CSA of satellite cell ablation as such, since SC−OL− muscles were similar to SC+OL− muscles.

As expected from the CSA averages, the CSA frequency distribution for the SC+OL+ group displayed a marked right shift (Fig. 3C) both in the plantaris and EDL. In the plantaris there were fewer fibers in the range 500-1800 µm^2 and generally more fibers above ≈2000 µm^2. The EDL had fewer fibers below ≈1200 µm^2 and more fibers in the range 1400-2600 µm^2 after overload.

For the EDL, the CSA distribution of all the groups other than the SC+OL+ group, were similar (Fig. 3C, right panel), suggesting that none of the other treatments had an effect; thus, there was apparently no effect of overload in the absence of satellite cells (SC−OL+), and SC ablation as such had no effect (SC−OL−).

In the plantaris, overload had an effect on the CSA distribution even in SC− muscles (Fig. 3C, left panel). Although there was no significant change in average CSA in response to overload, CSAs became more homogenous as overload led to fewer fibers below ≈1000 µm^2 and above ≈2000 µm^2. Thus, overload led to a narrower distribution of CSA size peaking at ≈1600 µm^2 in this muscle.

Muscle mass is dependent on factors other than fiber hypertrophy

Although the definition of hypertrophy is an increase in the size of pre-existing fibers, muscle mass is often used as a proxy for hypertrophy. We found that for the plantaris the overload surgery led to an increase in mass both with (112%) and without (55%) satellite cells (Fig. 4A, left panel). The EDL showed the same tendency, but the increase in the SC−OL+ group was not significant. The mass increases in the SC− muscles were not related to any increase of the CSA and for the SC+ plantaris the mass increase was much larger than the 26% increase in CSA.

We attribute the discrepancies between mass and CSA in the plantaris mainly to post-operative complications and difficulties in defining this muscle anatomically at the proximal end, particularly

Development (2016) 143, 2898-2906 doi:10.1242/dev.134411

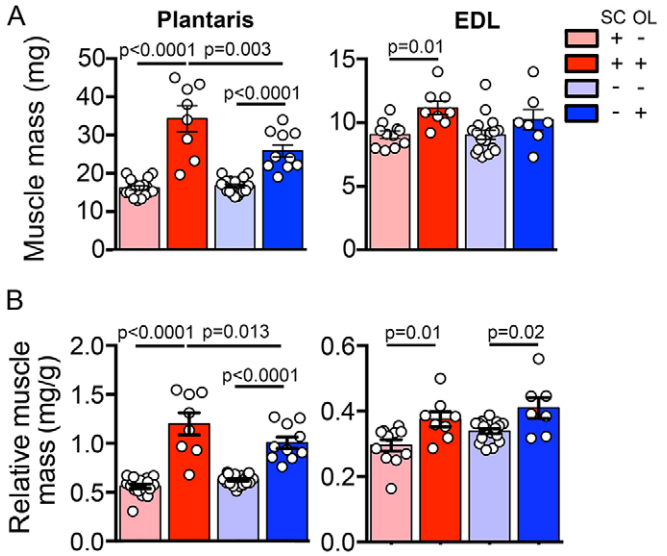

Fig. 4. The effect of overload on muscle mass. (A,B) Absolute muscle mass (A) or muscle mass relative to body weight (B) given as mean±s.e.m., and values from individual (circles) animals for plantaris (left panels) and EDL (right panels) muscles. Plantaris: SC+OL– *n*=17; SC+OL+ *n*=8; SC–OL– *n*=18; SC–OL+ *n*=10 animals. EDL: SC+OL– *n*=11; SC+OL+ *n*=8; SC–OL– *n*=17; SC–OL+ *n*=7 animals.

after synergist ablation. Microscopical analysis of sections frequently showed adhering tissue from other muscles after the excision. Thus, at the proximal end, plantaris fuses with the gastrocnemius and after ablation surgery adherences make it even more difficult to dissect out the plantaris in a precise manner. Histology on cross-sections showed that parts of gastrocnemius were frequently part of the 'lump' when the plantaris was dissected out from synergist-ablated animals. Thus, in our hands mass is an unreliable measure of hypertrophy in the plantaris overload model.

The EDL muscle was easier to excise after synergist ablation than the plantaris, but post-operative adherences were a problem even for this muscle. The increase in mass after overload in the SC+ group was 23%, similar to the increase in CSA (Fig. 4, right panel). The SC– group also had a slightly higher mass (13%) after overload, but this was not statistically significant. Thus, in the EDL there was a reasonably good agreement between the changes in mass and CSA.

In our study, tamoxifen-treated mice had on average a 13% lower body weight than sham-treated animals. When correcting for body weight, this would tend to increase the relative mass values for the tamoxifen groups (Fig. 4B). These body weight corrections might, however, represent an overcorrection, and hence a false hypertrophy as a major effect of this estrogen antagonist is to reduce body fat (Liu et al., 2015). McCarthy et al. reported only muscle mass corrected for body weight, not absolute muscle mass.

Overload hypertrophy is related to an increase in the number of myonuclei

Activation of SCs is thought to be important during hypertrophy in order to increase the number of myonuclei to match the increase in cytoplasmic volume. Thus, we investigated the number of myonuclei per fiber on histological cross-sections co-labeled with anti-dystrophin. Nuclei with their geometric center within the inner rim of the dystrophin ring were defined as myonuclei (Fig. 5A, arrows), and the number of these nuclei was divided by the number of fibers analyzed on the same section.

Overload of SC+ muscles led to a 51% increase in the number of myonuclei in the plantaris and 30% in the EDL (Fig. 5B). Thus, for the plantaris the increase was twice what would be expected from the 26% increase in cytoplasmic volume, whereas in the EDL the increase was more similar to the increase in cytoplasmic volume. In

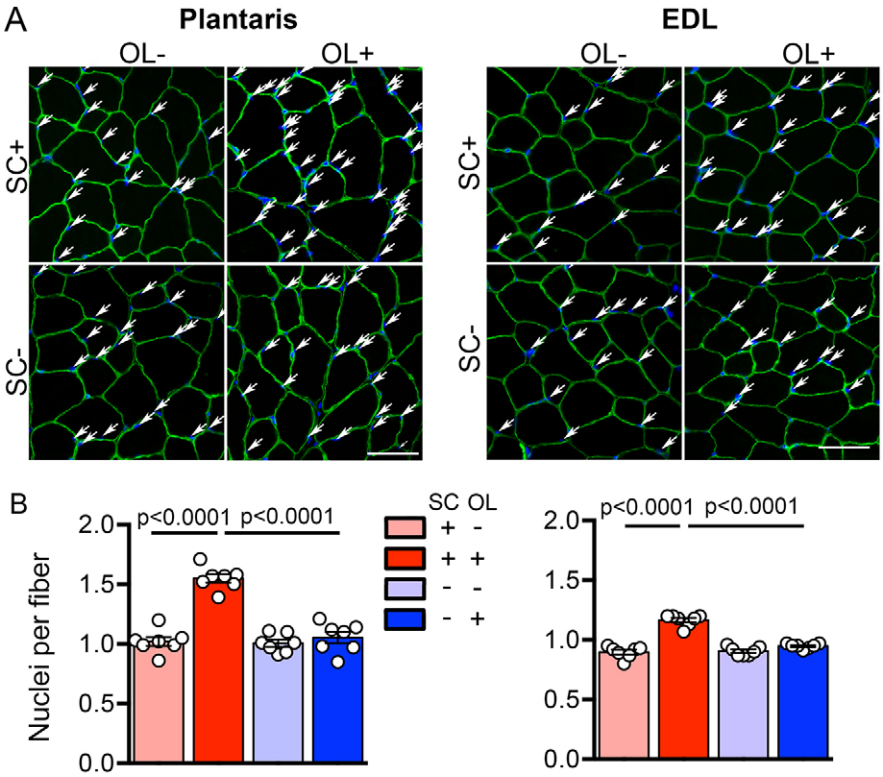

Fig. 5. The effect of overload on number of myonuclei determined from cross-sections. (A) Micrographs of cryosections from plantaris (left) and EDL (right), stained for DNA (blue) and dystrophin (green). Arrows indicate myonuclei. Scale bars: 50 µm. (B) Quantification of myonuclei per fiber from the plantaris (left) and EDL (right). Data are given as mean±s.e.m., and values from individual muscles (circles). *n*=7 animals in each group.

Development (2016) 143, 2898-2906 doi:10.1242/dev.134411

the SC− group, overload led to no significant change in the number of myonuclei in plantaris or EDL (Fig. 5B).

Identification of myonuclei on cross-sections can be unreliable (Bruusgaard et al., 2012; Bruusgaard and Gundersen, 2008; Gundersen and Bruusgaard, 2008). We therefore went on to study myonuclei in single fibers. For the plantaris, single fibers were teased out after maceration of fixed muscles (Fig. 6A). As in previous papers using this technique, there were differences between experimental groups in the degree of stretch (Bruusgaard et al., 2010); thus, number of nuclei is given per sarcomere length. The only group that showed an increase in this variable was the SC+OL+ group (Fig. 6B).

The most precise technique to observe the myonuclei belonging to a single fiber syncytium is *in vivo* imaging after intracellular injection of a nuclear dye. Although this is not feasible in the plantaris, surface fibers on the lateral side of EDL are well-suited for such analysis (Fig. 7A). When such fibers were analyzed *in vivo*, it was observed that overload led to a 60% increase in myonuclear number in the SC+ group (Fig. 7B), and the increase in CSA calculated from the *en face* diameter increased 34% (Fig. 7C). There was also on average a 19% increase in the number of myonuclei in the SC− group. This small increase could be related to residual SCs (McCarthy et al., 2011), but was apparently not sufficient to support any hypertrophy in our experiments (Fig. 7C).

The increase in the number of myonuclei was larger than the increase in cytoplasmic volume, thus in SC+OL+ muscles the myonuclear domain volume decreased by 22% (Fig. 7D). This might be related to the myonuclear recruitment preceding the radial growth as shown previously (Bruusgaard et al., 2010).

A significant correlation between CSA and nuclei per fiber length was observed in all the four experimental groups (Fig. 7E). The correlation was shifted to higher number of nuclei for the same CSA in SC+OL+ muscles. For the other groups, experimental conditions

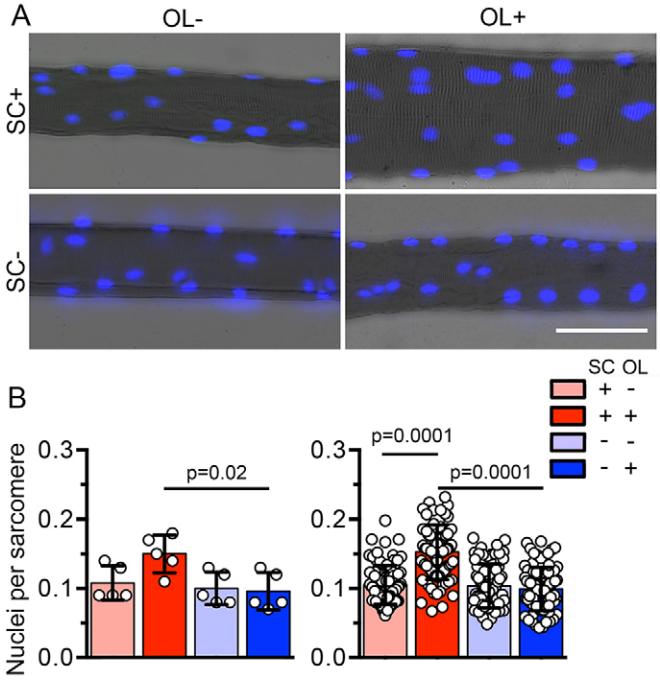

Fig. 6. The effect of overload on number of myonuclei in plantaris muscles determined from single macerated fibers. (A) Micrographs of macerated fibers from the plantaris muscle stained for DNA (blue). Scale bar: 50 µm. (B) Quantification of nuclei per sarcomere length. In the left panel, each circle represents average values for an individual muscle based on a sample of 8-32 fibers from each muscle. Columns denote mean±s.e.m. of five animals each. In the right panel, each circle represents the individual fibers in the same material. Columns denote mean±s.e.m. for all the fibers from five animals in each group. SC+OL− *n*=84; SC+OL+ *n*=89; SC−OL− *n*=76; SC−OL+ *n*=81.

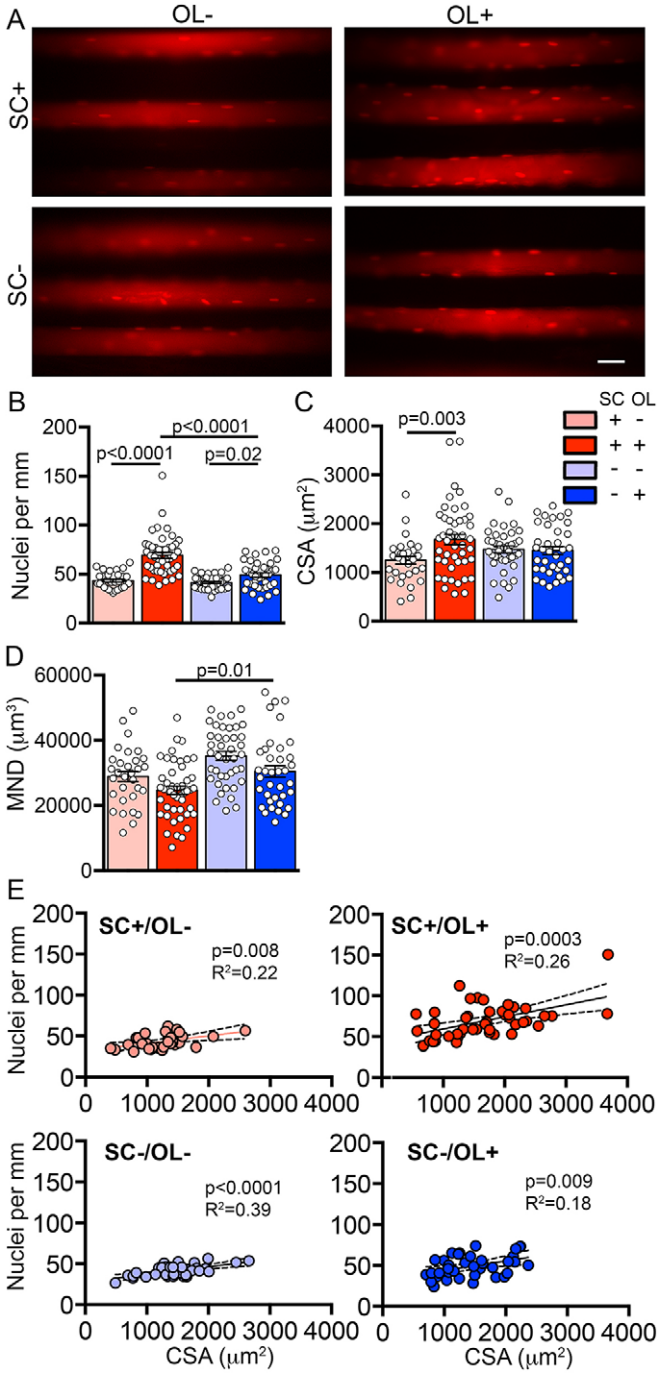

Fig. 7. The effect of overload on number of myonuclei in EDL determined by *in vivo* imaging of single fibers. (A) *In vivo* images of fibers injected with TRITC-labeled oligonucleotides displaying the myonuclei. *In situ* sarcomere length is ≈3.1 µm. Scale bar: 30 µm. (B-D) Quantification of myonuclei per fiber length (B), CSA (C) and myonuclear domain volume (MND) (D). Each circle represents the value from one fiber, SC+OL− *n*=31(4); SC+OL+ *n*=39(5); SC−OL− *n*=45(7); SC−OL+ *n*=37(7) (number of animals in parenthesis). Each column denotes the mean±s.e.m. of 31-45 fibers from four to seven animals. (E) Correlation between myonuclei per fiber length and CSA; each circle represents one fiber.

Development (2016) 143, 2898-2906 doi:10.1242/dev.134411

had little effect, except that the variability in the number of nuclei was larger in the OL+ groups (Fig. 7E, right-hand panels).

DISCUSSION

We show that ablation of satellite cells prevents overload hypertrophy and suggest that SC activation and subsequent fusion to muscle fibers resulting in an increase in the number of myonuclei is obligatory for normal hypertrophy.

The finding seems to support the long-standing notion of nuclear domains: that proteins are expressed locally in the vicinity of each nucleus (Gundersen et al., 1993; Merlie and Sanes, 1985; Ralston and Hall, 1992; Ralston et al., 1997; Sanes et al., 1991), and that each nucleus can support only a limited volume of cytoplasm (Gregory, 2001; Hall and Ralston, 1989; Strassburger, 1893). The relevant bottleneck relating the number of nuclei to cytoplasmic volume is not known, although it has been speculated that capacity for shuttling of macromolecules over the nuclear membrane could act as a limiting factor if the number of nuclei is not sufficiently high (Gundersen, 2016; Hall et al., 2011).

Our findings are in conflict with McCarthy et al. (2011) who used essentially the same approach as us. For both studies, the remaining satellite cell pool in overloaded SC− muscles was the same relative to normal muscles (SC+OL−), and was apparently sufficient to prevent an increase in the number of myonuclei when these muscles were overloaded. Therefore, we attribute the differences in the results to differences in the way hypertrophy was analyzed, such as the reliance on relative muscle mass as a proxy for fiber hypertrophy and the inclusion of regenerating fibers in the McCarthy study.

Muscle mass as a proxy for hypertrophy

McCarthy et al. (2011) based their conclusions mainly on changes in relative muscle mass as a proxy for hypertrophy. To some extent, we reproduced their findings using this variable, but because CSA did not increase along with the mass, we attribute this finding to confounding factors related to adherences and effects of the surgery rather than fiber hypertrophy (see Results).

McCarthy et al. (2011) did not report CSA averages, but from their CSA histogram we calculated that the average overload hypertrophy was ≈11% in SC+ muscles, and similarly so also in a more recent paper (Kirby et al., 2016). This is a rather narrow scope, considering it was compared to a ≈10% increase in the average CSA in their SC− muscles. We suggest that the apparent unblunted hypertrophy in the satellite cell-deficient group only appears robust because there was so little hypertrophy in the control muscles. In our overloaded controls (SC+OL+), by contrast, we observed an average increase in CSA of 26%, and this magnitude is in agreement with previous literature on short-term effects of plantaris overload by synergist ablation (e.g. White et al., 2009; Zhang et al., 2014). This robust SC+ hypertrophy gave us a sufficiently large scope for observing the attenuation of hypertrophy in SC− muscles.

Although subtle differences in genetic background or overload conditions might have played a role, for example we observed a higher number of satellite cells in our SC+OL+ muscles, we suggest that the differences in the CSA data of the SC+ plantaris muscles between the present study and that of McCarthy et al. (2011) can be attributed mainly to the degree of muscle damage and the inclusion criteria for the fibers analyzed.

Muscle damage and the inclusion criteria for the fibers analyzed

The plantaris overload model is rather extreme, as the relatively small plantaris muscle suddenly has to bear the load that was previously supported by both the soleus and the much larger gastrocnemius muscle, and this could lead to rupture damage of muscle fibers. In addition, the blood supply to the plantaris that comes through the gastrocnemius is easily damaged during a radical ablation of the gastrocnemius.

McCarthy et al. (2011) report that ∼30% of fibers in their SC+OL+ group expressed embryonic myosin and/or centrally located nuclei as signs of damage or regeneration. Importantly, the authors used automated CSA measurements and these regenerating/damaged fibers were included in their analysis. We observed that such fibers were generally smaller than fibers with normal morphology (compare Fig. 2E and Fig. 3C). Inclusion of a substantial population of such fibers would tend to shift the total CSA distribution to the left and hence explain the low degree of hypertrophy in their SC+OL+. This would apply to their SC+OL+ mice only, and not to the SC−OL+ mice. This would tend to mask a difference in the hypertrophy of pre-existing fibers between the two groups.

In contrast to McCarthy et al. (2011), we excluded fibers with signs of damage from our analysis. In any case, the number of such fibers was lower in our plantaris material, and in the EDL such fibers were rather rare so this confounding factor was not much of a problem in this muscle. EDL was not analyzed by McCarthy et al. (2011).

In a recent paper, the Peterson group (Fry et al., 2014) essentially repeated their previous experiments on the plantaris, but extended the overload time to 8 weeks. Their new data suggest a role for satellite cells in long-term hypertrophy as SC ablation attenuated the hypertrophy response from a 36% to a 26% increase in CSA. The latter increase seemed to occur without an increase in the number of myonuclei. This finding might be an example of a hypertrophy without an increase in the number of myonuclei, but the extensive initial tissue damage reported for the plantaris overload model by McCarthy et al. (2011), probably also applies to the experiments of Fry et al. (2014) since at 8 weeks 9% of the fibers still had central nuclei. Thus, the muscle history could be a confounding factor for interpretations related to hypertrophy of pre-existing fibers also for the Fry et al. (2014) study.

Is recruitment of SCs obligatory for hypertrophy?

Our data confirms most of the studies in which hypertrophy was prevented by γ-irradiation (Adams et al., 2002; Barton-Davis et al., 1999; Phelan and Gonyea, 1997; Rosenblatt and Parry, 1992; Rosenblatt et al., 1994). Are there then any remaining models suggesting that recruitment of myonuclei are not obligatory for functional hypertrophy?

Transgenic models related to myostatin inhibition display large fibers without a corresponding increase in the number of myonuclei (Amthor et al., 2009; Bruusgaard et al., 2005; Lee et al., 2012; Raffaello et al., 2010), but the hypertrophy seems not to be fully functional as the specific force is reduced in such muscles (Amthor et al., 2007; Charge et al., 2002; Mendias et al., 2011).

It has been suggested that the beta-agonist clenbuterol induces hypertrophy in rats without addition of myonuclei by satellite cell proliferation (Rehfeldt et al., 1994), but the assessment of myonuclei would have to be repeated with modern methods, and the functionality of the hypertrophy was not determined.

Hypertrophy without activation of satellite cells or increase in the number of myonuclei is induced by overexpression of the serine/threonine kinase Akt/PKB. Such muscle fibers seemed to have normal specific force after 3 weeks of overexpression (Blaauw et al., 2009), but it remains unclear if this condition is sustainable over longer periods (Blaauw and Reggiani, 2014).

Development (2016) 143, 2898-2906 doi:10.1242/dev.134411

In conclusion, a fully functional, sustainable, *de novo* hypertrophy without SC contribution remains to be unequivocally demonstrated.

The demonstration of the muscle memory phenomenon (Bruusgaard and Gundersen, 2008; Bruusgaard et al., 2010; Egner et al., 2013; for a review, see Gundersen, 2016), for which efficient re-growth relies on myonuclei recruited during a previous hypertrophic episode, is an important example of functional radial growth without the need for new myonuclei from satellite cells. This has been directly demonstrated using the hind limb suspension model, in which atrophy is induced by lifting up the hind part of rodents by the tail and thereby unloading the hind leg. Myonuclei are not lost during this atrophy. When the muscles were reloaded by letting the animal back down again the fibers displayed a 60% radial re-growth, and this re-growth was not accompanied by any increase in the number of myonuclei (Bruusgaard et al., 2012). Moreover, using a similar mouse model as used in the present study it was demonstrated that the re-growth was not affected by satellite cell ablation (Jackson et al., 2012). This notion is also supported by previous suggestions that until a certain limit of hypertrophy is reached, it can occur without recruiting new myonuclei (Kadi et al., 2005; Petrella et al., 2006, 2008), and we have suggested a 'peak pegging' hypothesis in which the number of myonuclei reflects the largest size a muscle fiber has had in its history (Gundersen, 2016). Thus, during re-growth satellite cells are not required, not because a large number of myonuclei is not needed in large fibers, but because the nuclei are already there. The present data indicate that recruitment of new myonuclei is obligatory for *de novo* hypertrophy.

MATERIALS AND METHODS

Animal experiments

All animal experiments were approved by the Norwegian Animal Research Authority and were conducted in accordance with the Norwegian Animal Welfare Act of 20 December 1974. The Norwegian Animal Research Authority provided governance to ensure that facilities and experiments were in accordance with the Animal Welfare Act; the National Regulations of 15 January 1996; and the European Convention for the Protection of Vertebrate Animals used for Experimental and Other Scientific Purposes of 18 March 1986.

Inhalation of gas anesthesia with 2% (vol/vol) isoflurane in air was used for all non-terminal experiments.

For terminal experiments, intraperitoneal injections at a dose of 10 µl/g body weight of a mixture of 18.7 mg/ml Zoletil Forte (Virbac Laboratories, France), 0.45 mg/ml Narcorxyl/Rompun (Bayer Animal Health, Germany) and 2.62 µg/ml Fentanyl (Hameln Pharmaceuticals, Germany) was used. All live animal imaging and surgery were performed under deep anesthesia checked regularly by pinching the metatarsus region of the limb. Additional doses were given if necessary.

A Pax7-DTA mouse strain that allows for conditional ablation of $Pax7^+$ cells was used for all experiments. This strain was generated by crossing the previously described (Murphy et al., 2011) strain B6.Cg-Pax7tm1(cre/ERT2)Gaka/J (Jackson Laboratory stock number: 017763) to the previously described (Wu et al., 2006) strain B6;129-Gt(ROSA)26Sortm1(DTA)Mrc/J (Jackson Laboratory stock number: 010527). Homozygous breeding pairs were used and correct genotype was confirmed by PCR according to the Jackson Laboratory protocol.

Mice were housed in a temperature- and humidity-controlled room and maintained on a 12:12 h light-dark cycle with food and water *ad libitum*.

Adult (3-4 months) female Pax7-DTA mice were randomly assigned to receive either an intraperitoneal injection of tamoxifen (Sigma-Aldrich, T5648-56) at a dose of 2.0 mg/day, or vehicle containing 10% ethanol in corn oil (Sigma-Aldrich, C8267) for 5 days, followed by a 2-week washout period. Following the 2-week washout period, mice were divided into either synergist ablation of the EDL or the plantaris muscle, or non-ablated control.

Overload of the plantaris muscle was induced by excising the distal half of both the gastrocnemius and the soleus. Overload of the EDL muscle was achieved by excising approximately two-thirds of the distal end of the tibialis anterior. Ablations were performed unilaterally, and all animals were subjected to 2 weeks of synergist ablation. Mice on which no surgery was performed served as controls (OL−).

Immunohistochemistry

The muscles were dissected free from surrounding connective tissue, weighed, and pinned to a rubber form at resting length, embedded in OCT Tissue-Tek (Sakura Finetek Europe B.V.), quickly frozen in melting isopentane, and stored at −80°C until sectioning. Muscles were cryosectioned at 10 µm, air dried and stored at −80°C. Before immunostaining, frozen sections were air-dried and subsequently blocked in 1% bovine serum albumin and incubated with primary antibodies at 4°C overnight and secondary antibodies for 1 h at room temperature. The following primary antibodies were used: anti-dystrophin (1:200; Abcam, ab15277), anti-MYH3 (1:50; Santa Cruz Biotechnology, sc53091) or anti-laminin (1:200; Sigma-Aldrich, L9393). After three 10 min washes in PBS, sections were incubated with secondary antibodies: goat anti-mouse IgG-TRITC (1:200; Sigma-Aldrich, T7782) or goat anti-rabbit IgG-FITC (1:200; Abcam, ab150077). Nuclei were co-stained using Hoechst dye 33342 (Invitrogen; 0.1 µg/ml in PBS).

Satellite cells were labeled by fixing in 2% paraformaldehyde for 5 min followed by epitope retrieval using a sodium citrate/TWEEN buffer (10 mM, pH 6.5, 0.05% TWEEN) at 95°C for 30 min. Sections were stained with primary antibodies against Pax7 (1:5 dilution in PBS, 2% BSA, 0.1% Triton X-100; Developmental Studies Hybridoma Study Bank, AB 528428) at 4°C overnight, and subsequently stained with secondary antibodies (1:200 dilution in PBS, 2% BSA; goat anti-mouse IgG Alexa Fluor 488, Thermo Fisher Scientific, A27012). All sections were counterstained with Hoechst 33342 to verify nuclear Pax7 staining. Sections were imaged using an Olympus BX-50WI fluorescence microscope with a 40×0.8 NA long working distance water immersion objective and an Andor iXion+ camera, controlled by Andor SOLIS software.

For sampling fibers for CSA quantification, a grid was placed over the images and fibers that were located in the grid intersections from all parts of the muscle were measured such that an average of 161 (range 101-205) were sampled from each whole muscle cross-section. For the sampled fibers, CSA was measured manually by circling the dystrophin ring. A set of images of each muscle was captured using an Olympus BX-50WI fluorescence microscope with a 40×0.8 NA long working distance water immersion objective and a Canon 60D SLR camera. As discussed previously (Bruusgaard et al., 2012; Gundersen and Bruusgaard, 2008), to ensure that only nuclei inside the sarcolemma (the myonuclei proper) were included in the analysis, myonuclei were defined as nuclei with their geometrical center inside the inner rim of the dystrophin ring. Fibers with centrally located nuclei and/or embryonic staining were excluded from the analysis.

In vivo myonuclear imaging

For *in vivo* labeling of myonuclei, single fibers in the EDL were injected with a solution containing a 5′-TRITC-labeled random 17-mer oligonucleotide with a phosphorothioated backbone (Yorkshire Biosciences) dissolved in an injection buffer (10 mM NaCl, 10 mM Tris, pH 7.5, 0.1 mM EDTA and 100 mM potassium gluconate). The oligonucleotides are taken up into the nuclei inside the injected fibers apparently by active transport, and serve solely as an intravital nuclear dye in our experiments. The methods have been described in detail previously (Bruusgaard et al., 2003; Utvik et al., 1999).

The oligonucleotides contained the randomly selected sequence TAGTCCTAAGTGGACGC, and a BLAST analysis confirmed that the sequence was not represented in the mouse genome either in the sense or antisense direction.

In vivo imaging was performed essentially as described previously (Balice-Gordon and Lichtman, 1994; Bruusgaard et al., 2010, 2003; Utvik et al., 1999). Fiber segments of 250-1000 µm were analyzed by acquiring images in

Development (2016) 143, 2898-2906 doi:10.1242/dev.134411

different focal planes 5 µm apart on an Olympus BX-50WI fluorescence microscope with a 20×0.5 NA long working distance water immersion objective. All images were acquired with an Andor iXion+ camera, controlled by Andor SOLIS software. By importing the images to a Macintosh computer running Adobe Photoshop and NIH ImageJ software, a stack was generated and used to count all the nuclei in the segment. The counting of nuclei was performed by evaluating all of the images in each stack.

Ex vivo single fiber analysis

The plantaris muscle was fixed in 4% paraformaldehyde (wt/vol) at 4°C for 48 h. The muscles were subsequently incubated in a 40% (wt/vol) NaOH solution for 2-3 h at room temperature, followed by shaking for 8 min in 20% (wt/vol) NaOH and three washes in dH_2O. Fibers were then transferred to a Petri dish with 5 ml dH_2O and stained with two or three droplets of Hematoxylin (Santa Cruz Biotechnology, sc-24973) for visualization of fibers and fiber structure. Watchmaker's forceps and a binocular microscope were then used to disperse single fibers on microscope slides (Superfrost Plus, Thermo Scientific, J1800AMNZ). For visualizing nuclei, fibers were mounted with ProLong Diamond Antifade Mountant with DAPI (Molecular Probes, P36962). Segments of 171-623 µm from 330 fibers were analyzed by acquiring images in different focal planes 5 µm apart on an Olympus BX-50WI fluorescence microscope with a 40×0.8-N.A. water immersion objective. Using ImageJ software (National Institutes of Health), a *z*-stack of the images were generated and Adobe Photoshop (Adobe Systems) were used for further measurements.

Statistics

Differences between groups were analyzed using GraphPad Prism software using one-way ANOVA statistical analysis with Holm–Sidak post-tests.

Acknowledgements

We are grateful to Dr Einar Eftestøl and Kenth-Arne Hansson for comments on the manuscript.

Competing interests

The authors declare no competing or financial interests.

Author contributions

I.M.E. and J.C.B. performed the experiments. J.C.B. prepared the figures. I.M.E., J.C.B. and K.G. designed the experiments. K.G. wrote the paper with input from I.M.E. and J.C.B.

Funding

This study was supported by the Research Council of Norway (Norges Forskningsråd) [grant 240374].

References

Adams, G. R., Caiozzo, V. J., Haddad, F. and Baldwin, K. M. (2002). Cellular and molecular responses to increased skeletal muscle loading after irradiation. *Am. J. Physiol. Cell Physiol.* **283**, C1182-C1195.

Allen, D. L., Monke, S. R., Talmadge, R. J., Roy, R. R. and Edgerton, V. R. (1995). Plasticity of myonuclear number in hypertrophied and atrophied mammalian skeletal muscle fibers. *J. Appl. Physiol.* **78**, 1969-1976.

Allen, D. L., Roy, R. R. and Edgerton, V. R. (1999). Myonuclear domains in muscle adaptation and disease. *Muscle Nerve* **22**, 1350-1360.

Aloisi, M., Mussini, I. Schiaffino, S. (1973). Activation of muscle nuclei in denervation and hypertrophy. In *Basic Research in Myology* (ed. B. A. Kakulas), pp. 338-345. Amsterdam: Exerpta Medica.

Amthor, H., Macharia, R., Navarrete, R., Schuelke, M., Brown, S. C., Otto, A., Voit, T., Muntoni, F., Vrbova, G., Partridge, T. et al. (2007). Lack of myostatin results in excessive muscle growth but impaired force generation. *Proc. Natl. Acad. Sci. USA* **104**, 1835-1840.

Amthor, H., Otto, A., Vulin, A., Rochat, A., Dumonceaux, J., Garcia, L., Mouisel, E., Hourde, C., Macharia, R., Friedrichs, M. et al. (2009). Muscle hypertrophy driven by myostatin blockade does not require stem/precursor-cell activity. *Proc. Natl. Acad. Sci. USA* **106**, 7479-7484.

Balice-Gordon, R. J. and Lichtman, J. W. (1994). Long-term synapse loss induced by focal blockade of postsynaptic receptors. *Nature* **372**, 519-524.

Barton-Davis, E. R., Shoturma, D. I. and Sweeney, H. L. (1999). Contribution of satellite cells to IGF-I induced hypertrophy of skeletal muscle. *Acta Physiol. Scand.* **167**, 301-305.

Blaauw, B. and Reggiani, C. (2014). The role of satellite cells in muscle hypertrophy. *J. Muscle Res. Cell Motil.* **35**, 3-10.

Blaauw, B., Canato, M., Agatea, L., Toniolo, L., Mammucari, C., Masiero, E., Abraham, R., Sandri, M., Schiaffino, S. and Reggiani, C. (2009). Inducible activation of Akt increases skeletal muscle mass and force without satellite cell activation. *FASEB J.* **23**, 3896-3905.

Bruusgaard, J. C. and Gundersen, K. (2008). In vivo time-lapse microscopy reveals no loss of murine myonuclei during weeks of muscle atrophy. *J. Clin. Invest.* **118**, 1450-1457.

Bruusgaard, J. C., Liestøl, K., Ekmark, M., Kollstad, K. and Gundersen, K. (2003). Number and spatial distribution of nuclei in the muscle fibres of normal mice studied in vivo. *J. Physiol.* **551**, 467-478.

Bruusgaard, J. C., Brack, A. S., Hughes, S. M. and Gundersen, K. (2005). Muscle hypertrophy induced by the Ski protein: cyto-architecture and ultrastructure. *Acta Physiol. Scand.* **185**, 141-149.

Bruusgaard, J. C., Johansen, I. B., Egner, I. M., Rana, Z. A. and Gundersen, K. (2010). Myonuclei acquired by overload exercise precede hypertrophy and are not lost on detraining. *Proc. Natl. Acad. Sci. USA* **107**, 15111-15116.

Bruusgaard, J. C., Egner, I. M., Larsen, T. K., Dupre-Aucouturier, S., Desplanches, D. and Gundersen, K. (2012). No change in myonuclear number during muscle unloading and reloading. *J. Appl. Physiol.* **113**, 290-296.

Cabrić, M. and James, N. T. (1983). Morphometric analyses on the muscles of exercise trained and untrained dogs. *Am. J. Anat.* **166**, 359-368.

Cabric, M., Appell, H.-J. and Resic, A. (1987). Effects of electrical stimulation of different frequencies on the myonuclei and fiber size in human muscle. *Int. J. Sports Med.* **8**, 323-326.

Charge, S. B. P., Brack, A. S. and Hughes, S. M. (2002). Aging-related satellite cell differentiation defect occurs prematurely after Ski-induced muscle hypertrophy. *Am. J. Physiol. Cell Physiol.* **283**, C1228-C1241.

Cheek, D. B., Holt, A. B., Hill, D. E. and Talbert, J. L. (1971). Skeletal muscle cell mass and growth: the concept of the deoxyribonucleic acid unit. *Pediatr. Res.* **5**, 312-328.

Egner, I. M., Bruusgaard, J. C., Eftestøl, E. and Gundersen, K. (2013). A cellular memory mechanism aids overload hypertrophy in muscle long after an episodic exposure to anabolic steroids. *J. Physiol.* **591**, 6221-6230.

Enesco, M. and Puddy, D. (1964). Increase in the number of nuclei and weight in skeletal muscle of rats of various ages. *Am. J. Anat.* **114**, 235-244.

Eriksson, A., Kadi, F., Malm, C. and Thornell, L.-E. (2005). Skeletal muscle morphology in power-lifters with and without anabolic steroids. *Histochem. Cell Biol.* **124**, 167-175.

Fry, C. S., Lee, J. D., Jackson, J. R., Kirby, T. J., Stasko, S. A., Liu, H., Dupont-Versteegden, E. E., McCarthy, J. J. and Peterson, C. A. (2014). Regulation of the muscle fiber microenvironment by activated satellite cells during hypertrophy. *FASEB J.* **28**, 1654-1665.

Giddings, C. J. and Gonyea, W. J. (1992). Morphological observations supporting muscle fiber hyperplasia following weight-lifting exercise in cats. *Anat. Rec.* **233**, 178-195.

Gollnick, P. D., Timson, B. F., Moore, R. L. and Riedy, M. (1981). Muscular enlargement and number of fibers in skeletal muscles of rats. *J. Appl. Physiol. Respir. Environ. Exerc. Physiol.* **50**, 936-943.

Gregory, T. R. (2001). Coincidence, coevolution, or causation? DNA content, cell size, and the C-value enigma. *Biol. Rev. Camb. Philos. Soc.* **76**, 65-101.

Gundersen, K. (2011). Excitation-transcription coupling in skeletal muscle: the molecular pathways of exercise. *Biol. Rev. Camb. Philos. Soc.* **86**, 564-600.

Gundersen, K. (2016). Muscle memory and a new cellular model for muscle atrophy and hypertrophy. *J. Exp. Biol.* **219**, 235-242.

Gundersen, K. and Bruusgaard, J. C. (2008). Nuclear domains during muscle atrophy: nuclei lost or paradigm lost? *J. Physiol.* **586**, 2675-2681.

Gundersen, K., Sanes, J. R. and Merlie, J. P. (1993). Neural regulation of muscle acetylcholine receptor epsilon- and alpha- subunit gene promoters in transgenic mice. *J. Cell Biol.* **123**, 1535-1544.

Hall, Z. W. and Ralston, E. (1989). Nuclear domains in muscle cells. *Cell* **59**, 771-772.

Hall, M. N., Corbett, A. H. and Pavlath, G. K. (2011). Regulation of nucleocytoplasmic transport in skeletal muscle. *Curr. Top. Dev. Biol.* **96**, 273-302.

Herbst, K. L. and Bhasin, S. (2004). Testosterone action on skeletal muscle. *Curr. Opin. Clin. Nutr. Metab. Care* **7**, 271-277.

Jackson, J. R., Mula, J., Kirby, T. J., Fry, C. S., Lee, J. D., Ubele, M. F., Campbell, K. S., McCarthy, J. J., Peterson, C. A. and Dupont-Versteegden, E. E. (2012). Satellite cell depletion does not inhibit adult skeletal muscle regrowth following unloading-induced atrophy. *Am. J. Physiol. Cell Physiol.* **303**, C854-C861.

Kadi, F., Eriksson, A., Holmner, S., Butler-Browne, G. S. and Thornell, L.-E. (1999). Cellular adaptation of the trapezius muscle in strength-trained athletes. *Histochem. Cell Biol.* **111**, 189-195.

Kadi, F., Charifi, N., Denis, C., Lexell, J., Andersen, J., Schjerling, P., Olsen, S. and Kjaer, M. (2005). The behaviour of satellite cells in response to exercise: what have we learned from human studies? *Pflügers Arch.* **451**, 319-327.

Kirby, T. J., Patel, R. M., McClintock, T. S., Dupont-Versteegden, E. E., Peterson, C. A. and McCarthy, J. J. (2016). Myonuclear transcription is responsive to mechanical load and DNA content but uncoupled from cell size during hypertrophy. *Mol. Biol. Cell* **27**, 788-798.

Development (2016) 143, 2898-2906 doi:10.1242/dev.134411

Lee, S.-J., Huynh, T. V., Lee, Y.-S., Sebald, S. M., Wilcox-Adelman, S. A., Iwamori, N., Lepper, C., Matzuk, M. M. and Fan, C.-M. (2012). Role of satellite cells versus myofibers in muscle hypertrophy induced by inhibition of the myostatin/activin signaling pathway. *Proc. Natl. Acad. Sci. USA* **109**, E2353-E2360.

Lipton, B. H. and Schultz, E. (1979). Developmental fate of skeletal muscle satellite cells. *Science* **205**, 1292-1294.

Liu, L., Zou, P., Zheng, L., Linarelli, L. E., Amarell, S., Passaro, A., Liu, D. and Cheng, Z. (2015). Tamoxifen reduces fat mass by boosting reactive oxygen species. *Cell Death Dis.* **6**, e1586.

Lowe, D. A. and Alway, S. E. (1999). Stretch-induced myogenin, MyoD, and MRF4 expression and acute hypertrophy in quail slow-tonic muscle are not dependent upon satellite cell proliferation. *Cell Tissue Res.* **296**, 531-539.

MacDougall, J. D., Sale, D. G., Alway, S. E. and Sutton, J. R. (1984). Muscle fiber number in biceps brachii in bodybuilders and control subjects. *J. Appl. Physiol. Respir. Environ. Exerc. Physiol.* **57**, 1399-1403.

McCall, G. E., Allen, D. L., Linderman, J. K., Grindeland, R. E., Roy, R. R., Mukku, V. R. and Edgerton, V. R. (1998). Maintenance of myonuclear domain size in rat soleus after overload and growth hormone/IGF-I treatment. *J. Appl. Physiol.* **84**, 1407-1412.

McCarthy, J. J. and Esser, K. A. (2007). Counterpoint: satellite cell addition is not obligatory for skeletal muscle hypertrophy. *J. Appl. Physiol.* **103**, 1100-1102; discussion 1102-3.

McCarthy, J. J., Mula, J., Miyazaki, M., Erfani, R., Garrison, K., Farooqui, A. B., Srikuea, R., Lawson, B. A., Grimes, B., Keller, C. et al. (2011). Effective fiber hypertrophy in satellite cell-depleted skeletal muscle. *Development* **138**, 3657-3666.

Mendias, C. L., Kayupov, E., Bradley, J. R., Brooks, S. V. and Claflin, D. R. (2011). Decreased specific force and power production of muscle fibers from myostatin-deficient mice are associated with a suppression of protein degradation. *J. Appl. Physiol.* **111**, 185-191.

Merlie, J. P. and Sanes, J. R. (1985). Concentration of acetylcholine receptor mRNA in synaptic regions of adult muscle fibres. *Nature* **317**, 66-68.

Moss, F. P. (1968). The relationship between the dimensions of the fibres and the number of nuclei during normal growth of skeletal muscle in the domestic fowl. *Am. J. Anat.* **122**, 555-563.

Moss, F. P. and Leblond, C. P. (1970). Nature of dividing nuclei in skeletal muscle of growing rats. *J. Cell Biol.* **44**, 459-462.

Murphy, M. M., Lawson, J. A., Mathew, S. J., Hutcheson, D. A. and Kardon, G. (2011). Satellite cells, connective tissue fibroblasts and their interactions are crucial for muscle regeneration. *Development* **138**, 3625-3637.

Petrella, J. K., Kim, J.-s., Cross, J. M., Kosek, D. J. and Bamman, M. M. (2006). Efficacy of myonuclear addition may explain differential myofiber growth among resistance-trained young and older men and women. *Am. J. Physiol. Endocrinol. Metab.* **291**, E937-E946.

Petrella, J. K., Kim, J.-s., Mayhew, D. L., Cross, J. M. and Bamman, M. M. (2008). Potent myofiber hypertrophy during resistance training in humans is associated with satellite cell-mediated myonuclear addition: a cluster analysis. *J. Appl. Physiol.* **104**, 1736-1742.

Phelan, J. N. and Gonyea, W. J. (1997). Effect of radiation on satellite cell activity and protein expression in overloaded mammalian skeletal muscle. *Anat. Rec.* **247**, 179-188.

Raffaello, A., Milan, G., Masiero, E., Carnio, S., Lee, D., Lanfranchi, G., Goldberg, A. L. and Sandri, M. (2010). JunB transcription factor maintains skeletal muscle mass and promotes hypertrophy. *J. Cell Biol.* **191**, 101-113.

Ralston, E. and Hall, Z. W. (1992). Restricted distribution of mRNA produced from a single nucleus in hybrid myotubes. *J. Cell Biol.* **119**, 1063-1068.

Ralston, E., McLaren, R. S. and Horowitz, J. A. (1997). Nuclear domains in skeletal myotubes: the localization of transferrin receptor mRNA is independent of its half-life and restricted by binding to ribosomes. *Exp. Cell Res.* **236**, 453-462.

Rehfeldt, C., Weikard, R. and Reichel, K. (1994). [The effect of the beta-adrenergic agonist clenbuterol on the growth of skeletal muscles of rats]. *Arch. Tierernahr.* **45**, 333-344.

Rosenblatt, J. D. and Parry, D. J. (1992). Gamma irradiation prevents compensatory hypertrophy of overloaded mouse extensor digitorum longus muscle. *J. Appl. Physiol.* **73**, 2538-2543.

Rosenblatt, J. D. and Parry, D. J. (1993). Adaptation of rat extensor digitorum longus muscle to gamma irradiation and overload. *Pflügers Arch.* **423**, 255-264.

Rosenblatt, J. D., Yong, D. and Parry, D. J. (1994). Satellite cell activity is required for hypertrophy of overloaded adult rat muscle. *Muscle Nerve* **17**, 608-613.

Roy, R. R., Monke, S. R., Allen, D. L. and Edgerton, V. R. (1999). Modulation of myonuclear number in functionally overloaded and exercised rat plantaris fibers. *J. Appl. Physiol.* **87**, 634-642.

Sanes, J. R., Johnson, Y. R., Kotzbauer, P. T., Mudd, J., Hanley, T., Martinou, J. C. and Merlie, J. P. (1991). Selective expression of an acetylcholine receptor-lacZ transgene in synaptic nuclei of adult muscle fibers. *Development* **113**, 1181-1191.

Schiaffino, S., Bormioli, S. P. and Aloisi, M. (1976). The fate of newly formed satellite cells during compensatory muscle hypertrophy. *Virchows Arch.* **21**, 113-118.

Seiden, D. (1976). Quantitative analysis of muscle cell changes in compensatory hypertrophy and work-induced hypertrophy. *Am. J. Anat.* **145**, 459-465.

Strassburger, E. (1893). Über die Wirkungssphäre der kerne und die zellgrösse. *Histol. Beitr.* **5**, 97-124.

Taylor, N. A. S. and Wilkinson, J. G. (1986). Exercise-induced skeletal muscle growth. Hypertrophy or hyperplasia? *Sports Med.* **3**, 190-200.

Utvik, J. K., Nja, A. and Gundersen, K. (1999). DNA injection into single cells of intact mice. *Hum. Gene Ther.* **10**, 291-300.

White, J. P., Reecy, J. M., Washington, T. A., Sato, S., Le, M. E., Davis, J. M., Wilson, L. B. and Carson, J. A. (2009). Overload-induced skeletal muscle extracellular matrix remodelling and myofibre growth in mice lacking IL-6. *Acta Physiol.* **197**, 321-332.

White, R. B., Biérinx, A.-S., Gnocchi, V. F. and Zammit, P. S. (2010). Dynamics of muscle fibre growth during postnatal mouse development. *BMC Dev. Biol.* **10**, 21.

Winchester, P. K. and Gonyea, W. J. (1992). A quantitative study of satellite cells and myonuclei in stretched avian slow tonic muscle. *Anat. Rec.* **232**, 369-377.

Wu, S., Wu, Y. and Capecchi, M. R. (2006). Motoneurons and oligodendrocytes are sequentially generated from neural stem cells but do not appear to share common lineage-restricted progenitors in vivo. *Development* **133**, 581-590.

Zhang, Q., Joshi, S., Lovett, D., Zhang, B., Bodine, S., Kim, H. and Liu, X. (2014). Matrix metalloproteinase-2 plays a critical role in overload induced skeletal muscle hypertrophy. *Muscles Ligaments Tendons J.* **4**, 362-370.